Methods and Applications in Fluorescence

The innards of the cell: studies of water dipolar relaxation using the ACDAN fluorescent probe.

To cite this article before publication: Santiago Otaiza-González *et al* 2022 *Methods Appl. Fluoresc.* in press https://doi.org/10.1088/2050-6120/ac8d4c

The innards of the cell: studies of water dipolar relaxation using the ACDAN fluorescent probe.

Santiago Otaiza-González[a], Manuel Cabadas[a], German Robert[b,c], Roberto P. Stock[d,*], Leonel Malacrida[e,f,*], Ramiro Lascano[b,c, *], and Luis A. Bagatolli[a,d,g †]

[a]Instituto de Investigación Médica Mercedes y Martín Ferreyra - INIMEC (CONICET) - Universidad Nacional de Córdoba, Friuli 2434, 5016, Córdoba, Argentina.
[b]Unidad Ejecutora de Doble Dependencia INTA-CONICET (UDEA), Córdoba, Argentina
[c]Cátedra de Fisiología Vegetal, Facultad de Ciencias Exactas, Físicas y Naturales. Universidad Nacional de Córdoba, Córdoba, Argentina.
[d]MEMPHYS - International and Interdisciplinary research network.
[e]Departamento de Fisiopatología, Hospital de Clínicas, Facultad de Medicina, Universidad de la República, Montevideo, Uruguay
[f]Advanced Bioimaging Unit, Institut Pasteur of Montevideo and Universidad de la República, Montevideo, Uruguay.
[g]Departamento de Química Biológica Ranwel Caputto, Facultad de Ciencias Químicas, Universidad Nacional de Córdoba, Córdoba, Argentina.

† In memory of our cherished friend Luis A. Bagatolli, the original corresponding author and driving force of these investigations, who passed away between submission and acceptance of this article.

*Correspondence to lmalacrida@pasteur.edu.uy/lmalacrida@hc.edu.uy

Abstract

This article reviews the use of the 6-acetyl-2-(dimethylamino)naphthalene (ACDAN) fluorophore to study dipolar relaxation in cells, tissues, and biomimetic systems. As the most hydrophilic member of the 6-acyl-2-(dimethylamino)naphthalene series, ACDAN markedly partitions to aqueous environments. In contrast to 6-lauroyl-2-(dimethylamino)naphthalene (LAURDAN), the hydrophobic and best-known member of the series used to explore relaxation phenomena in biological (or biomimetic) membranes, ACDAN allows mapping of spatial and temporal water dipolar relaxation in cytosolic and intra-organelle environments of the cell. This is also true for the 6-propionyl-2-(dimethylamino)naphthalene (PRODAN) derivative which, unlike LAURDAN, partitions to both hydrophobic and aqueous environments. We will i) summarize the mechanism which underlies the solvatochromic properties of the DAN probes, ii) expound on the importance of water relaxation to understand the intracellular environment, iii) discuss technical aspects of the use of ACDAN in eukaryotic cells and some specialized structures, including liquid condensates arising from processes leading to liquid immiscibility and, iv) present some novel studies in plant cells and tissues which demonstrate the kinds of information that can be uncovered using this approach to study dipolar relaxation in living systems.

Keywords: crowding; plant tissue; cytosol, water activity; spectral phasor analysis; GP function, Association Induction Hypothesis.

1. Introduction

As Gregorio Weber anticipated in his seminal 1979 article [1], 6-acyl-2-(dimethylamino)naphthalene (DAN) fluorescent probes have become useful tools to study nanosecond relaxation processes in biological systems. That year Weber rationally synthesized 6-propionyl-2-(dimethylamino)naphthalene (PRODAN) and presented a study of its interaction with bovine serum albumin, proposing the use of this type of fluorophores as "relaxation probes of various biological environments" [1]. In the same paper, Weber introduced two more DAN derivatives: 6-lauroyl-2-(dimethylamino)naphthalene (LAURDAN) and 6-acetyl-2-(dimethylamino)naphthalene (ACDAN). The structures of the three fluorophores are presented in Figure 1.

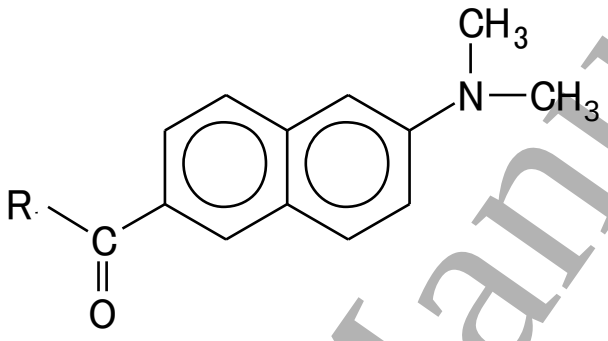

R	Acronymus
CH_3-	ACDAN
CH_3-CH_2-	PRODAN
CH_3-$(CH_2)_{10}$-	LAURDAN

Figure 1. Chemical structures of the first three 2,6-substituted naphthalene derivatives.

More DAN derivatives were designed and synthesized by Weber and others during the first half of the '80s with the purpose of probing dipolar relaxation in proteins. For example, 6'-(N,N-dimethyl)amino-2-naphtophyl-4-trans-cyclohexanoic acid (DANCA) was synthesized in Weber's lab and used to determine the polarity of the myoglobin heam pocket [2]. Later, Prendergast *et al*. synthesized 6-acryloyl-2-dimethylaminonaphtalene (ACRYLODAN), a 6,2-substituted naphthalene that selectively labels thiol moieties in proteins, to study dipolar relaxation in ubiquitous hydrophobic domains and protein conformational changes [3]. By the end of the '80s and throughout the following decade similar strategies were applied to the study of dipolar relaxation in membranes, both biomimetic and biological. This involved the extensive use and characterization of LAURDAN [4-

11] (the best known member of the DAN family) and, to a lesser extent, of PRODAN [10, 12] together with another newly synthesized probe, [6-palmitoyl-2-[[(2-trimethylammonium)ethyl]methyl]amino] naphthalene (PATMAN) [13, 14]. 6-dodecanoyl-2-[N-methyl-N-(carboxymethyl)amino] naphthalene (C-LAURDAN), a novel LAURDAN derivative, was synthesized some years later to explore the lateral structure of biological membranes in cells using fluorescence microscopy [15, 16]. Since then, more LAURDAN derivatives with longer hydrophobic tails (14, 16 and 18 carbons) were introduced allowing further studies of the regulation of membrane fluidity by the intracellular distribution of free fatty acids [17].

Only one paper using ACDAN [18] was published between its introduction in 1979 and 2015: a study of the effect of ethanol-induced lipid interdigitation on the solubility of ACDAN, PRODAN and LAURDAN in dipalmitoylphosphatidylcholine (DPPC) membranes that also compared their hydrophobicities by studying their partitioning into lipid membranes. As could be expected from their chemical structure, LAURDAN (the most hydrophobic) partitions exclusively to membranes, PRODAN is found in both membranes and water and ACDAN, the most hydrophilic, exhibits the greatest preference for aqueous phases with negligible partition to membranes [18]. In 2015 ACDAN and PRODAN were proposed as tools to measure dipolar relaxation in the cell cytosol [19-21], expanding the unique capabilities offered by LAURDAN in cell membranes to the rest of the intracellular environment. This proposal was linked to an experimental proof-of-concept of a theory of cell physiology called the Association-Induction Hypothesis (AIH; see section 3) [22]. Briefly, the AIH posits that interaction of the products of metabolism (e.g. ATP, hormones) with fibrillar proteins in the intracellular environment polarizes water by inductive effects, modulating its rotational dynamics with important consequences for cellular behavior. This theory has been extensively examined in suspensions of the yeast *Saccharomyces cerevisiae* under conditions of oscillatory glycolysis [19-21, 23-25].

The purpose of this article is to review methodological and technical aspects of applications making use of ACDAN to monitor the dynamics of intracellular water in various biological systems (yeast, mammalian and plant cells and organelles, and liquid condensates). We will also address the importance of water relaxation in the characterization of biological systems, including new data from our lab in plant cells and tissues, which illustrate the utility of this mostly unexplored parameter.

2. Theoretical considerations

2.1. A general mechanism of the response of DAN probes to dipolar relaxation in biological systems.

The most detailed mechanism explaining the behavior of the DAN probes was originally proposed by T. Parasassi and E. Gratton for LAURDAN [4, 6, 7] and PRODAN [12] inserted in lipid membranes (reviewed in [10, 11]). When labeled membranes undergo a solid ordered (s_o) to liquid disordered (l_d) phase transition, the probes shift their emission by ~50 nm [5-7]. Since the change in the "static" dielectric constant between the s_o and l_d phases is not sufficient to explain the observed fluorescence emission shift (in a classical sense following Lippert theory [26]), an alternative model was developed which incorporates the phenomenon of dipolar relaxation exerted by water [7]. Relaxation times were measured for LAURDAN in the l_d and s_o phases using an expression equivalent to the classical polarization equation by Perrin, the generalized polarization function (GP; see section 3.2) assuming a two state process [8] and determined to be 2.5×10^9 sec^{-1} and 4×10^7 sec^{-1} respectively. Since the fluorescence lifetime of the probe (~3×10^{-9} sec) and its relaxation time in the l_d phase occur in the same (nanosecond) time window, this suggested that this was the origin of the emission shift. Consequently, it was proposed that during the s_o to l_d phase transition the change in relaxation is operated by the presence of water molecules with restricted (rotational) mobility in the region where the probe is located (near the glycerol backbone of the glycerophospholipids) [6-8, 10, 11]. These membrane-associated water molecules have different dynamical properties than water molecules existing in bulk liquid water, which have an orientational (rotational) relaxation time below picoseconds. During the s_o to l_d phase transition part of the energy of the probe's transition moment reorients the membrane-associated water dipoles around it, lowering the energy of the excited state (S_1) and shifting the emission spectrum to longer wavelengths. The mechanism is sketched in Figure 2.

By now there is considerable experimental evidence for this mechanism as reviewed in [10, 11]. For example, experiments in LAURDAN-labeled dimyristoylphosphatidylcholine (DMPC) membranes in D_2O show slower relaxation dynamics at and above the s_o to l_d phase transition [10], although the main phase transition temperature is the same as in DMPC membranes prepared in H_2O. This important observation indicates that the greater mass of the ensemble of (membrane-associated) D_2O molecules reorienting as the supramolecular structure changes is enough to preclude a larger emission red shift during the s_o to l_d phase transition, as happens in the aqueous medium. Also, in agreement with the water dipolar relaxation model described above is another study which included the synthesis of three more hydrophobic DAN molecules: 2-methoxy-6-lauroylnapthalene (LAURMEN), 2-

hydroxy-6-lauroylnapthalene (LAURNA) and 2-diisopropylamino-6-lauroylnaphthalene (LAURISAN) [10]. A comparison of the behavior of LAURMEN, LAURNA and LAURISAN with LAURDAN showed not only the pivotal role of the charge transfer state to explain the shift but also ruled out the notion that the fluorophore itself (by intramolecular relaxation) was the cause of it [10].

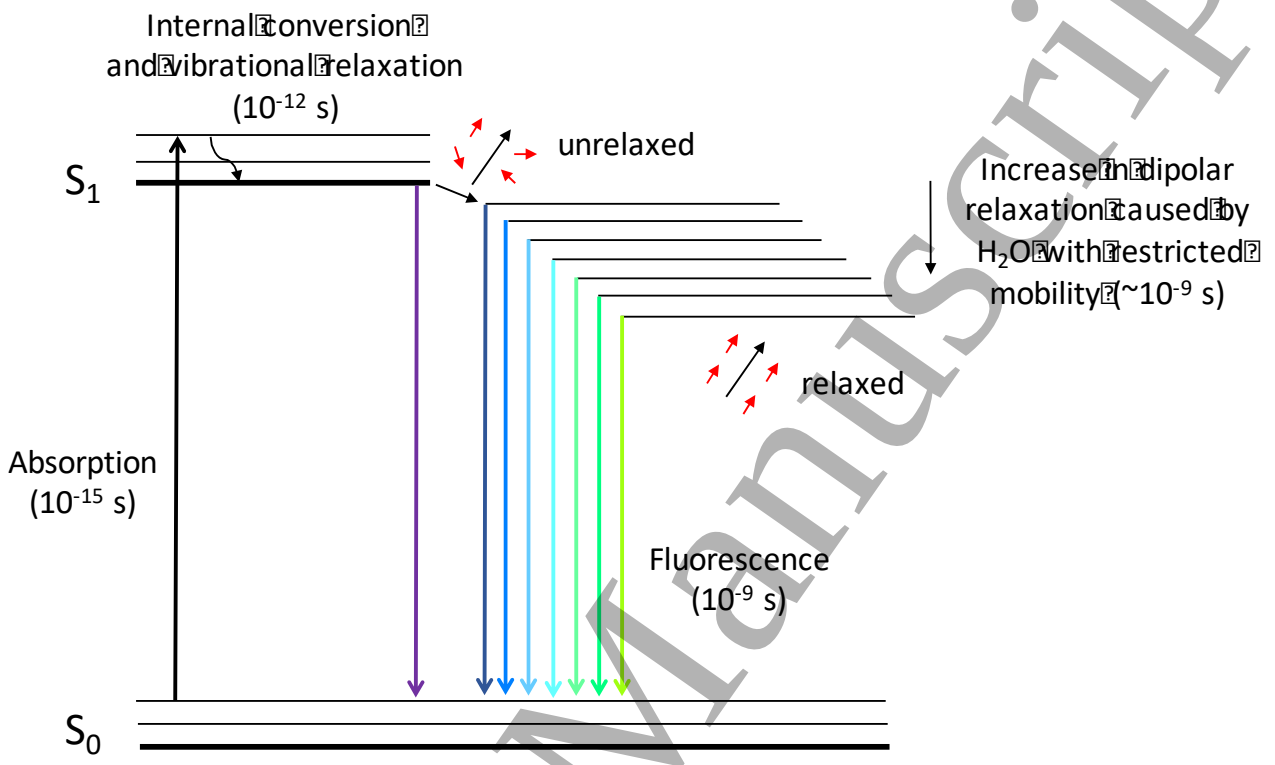

Figure 2. Simplified Perrin-Jabloński diagram showing the absorption and fluorescence processes occurring between the ground (S_0) and excited state (S_1) energy levels in the presence of solvent dipolar relaxation. S_1 decreases in energy as solvent dipolar relaxation proceeds during the nanosecond fluorescence lifetime of the probes (see text).

The mechanism is not exclusive for LAURDAN (and PRODAN) inserted in membranes; it can be generalized to the responses of ACDAN and PRODAN in the extremely crowded, non-membranous aqueous portion of the intracellular environment [19, 20]. The distinct hydrophilic-hydrophobic characteristics of the DAN probes have allowed studies of water dipolar relaxation in the intracellular milieu which discriminate between lipid-rich environments and the cytosol [19-21]. As mentioned in the introduction, the initial choice to use ACDAN (and PRODAN) as a relaxation probe to monitor the cell cytosol was determined by a colloidal model of the cell, specifically the AIH [22]. Therefore, it is important to first discuss why a parameter connected to the dynamics of intracellular water could be relevant to an understanding of the cellular interior. This is significant since cell water is usually taken to be a mostly passive solvent in our current view of the cell. In the next section we will briefly

examine some key aspects of the AIH [22], particularly its treatment of the behavior of intracellular water. We will accordingly review some relevant results using ACDAN that strongly argue in favor of the study of water dipolar relaxation to deepen our understanding of active processes in living cells and tissues.

2.2. Water as a key active component in the intracellular milieu

The DAN probes inform on the rotational freedom of cell water. Since the physicochemical properties of intracellular water are largely absent in discussions of cellular activity, we will take a brief detour to examine the reasons why we think they are relevant to understand the cellular interior. When studying suspensions of *Saccharomyces cerevisiae* displaying glycolytic oscillations, a very strong coupling between the fluorescence responses of the DAN probes and the oscillating activity of ATP and NADH was uncovered. Specifically, the quantum yield and Generalized Polarization (GP) function of ACDAN and PRODAN (and also LAURDAN) oscillate with the very same frequency as the chemical oscillations of the central metabolites of glycolysis [19, 20, 23], as shown in Figure 3. Additional experiments with ACDAN (and PRODAN) using D_2O in oscillating cells, which included an assessment of the response of the probes to artificial crowding agents (which decrease water activity, e.g. PEG), lent further support to the idea that the DAN fluorescence oscillations arise from periodic changes in the dipolar (rotational) relaxation of water, the most abundant component of the cell in both mass and number [19]. Importantly, this study established that the measured changes in dipolar relaxation are scale-independent, behaving as an intensive property of the cell [19]. In addition, this parameter was shown to be key for the emergence of the glycolytic oscillations themselves [20]. This physico-chemical coupling, which revolves around the concentration of ATP and is strictly dependent on the integrity of the actin cytoskeleton [19, 20], extends to other cellular properties such as pH, K^+ activity, temperature, volume and heat capacity [21, 24].

Taken together the results strongly support the existence of general cell-wide coupling principles, suggesting that metabolic processes influence and are influenced by the physical properties of the intracellular environment, which is cyclically altered by the accumulation/disappearance of central products of metabolic reactions (e.g. ATP). This in turn points to a role for water which has hitherto not been considered in the classical models that interpret metabolic oscillations, and other cellular functions, in terms of kinetic (diffusional) aspects of enzymes implicitly taken to be acting in mostly isotropic environments akin to dilute solutions.

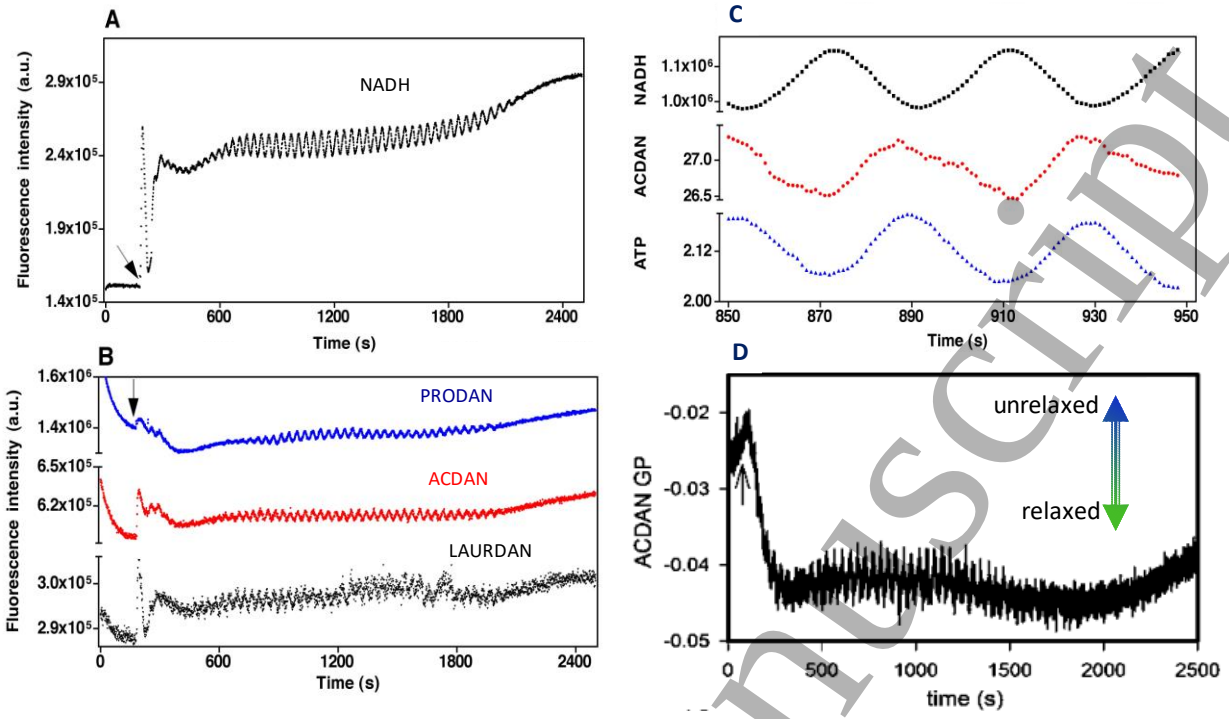

Figure 3. (A) Temporal oscillations of NADH fluorescence. (B) Temporal oscillations in the fluorescence emission of the DAN series observed during the metabolic oscillations. (C) Temporal oscillations of NADH, ACDAN and ATP. ATP is expressed in mM and is measured with an aptamer-based nanosensor; NADH and ACDAN are fluorescence counts. (D) Oscillations in ACDAN GP during glycolytic oscillations. The amplitude of the GP oscillations denotes cyclic transitions from relaxed to unrelaxed states. Adapted from [19, 20]

It is clear from these considerations that the classical view of the cell, with its lack of a theoretical treatment of the properties –at the relevant scales– of intracellular water, may not be adequate to explain this physicochemical coupling. It can, however, be productively approached using the theoretical bases of the AIH [22, 27]. This theory of cell physiology, which rigorously develops a wholly novel conceptual approach based on well-established principles of colloidal physical chemistry and statistical mechanics, provides a general explanatory framework for how the emergent properties of the intracellular environment are coupled to metabolism [28, 29]. Specifically, regarding the physical state of intracellular water, the AIH incorporates a subsidiary theory called Polarized-Oriented Multilayer Theory of Cell Water [22, 30] which develops the idea that the backbones of protein chains in extended states (fibrillar conformations of cytoskeletal proteins and/or intrinsically disordered proteins; IDPs) exhibit regularly spaced groups with negative and positive charge density (called NP systems). These regularly spaced sites orient and polarize successive layers

of water dipoles with opposite orientations, resulting in a dynamical regulation of water rotational freedom dependent on protein conformations. The supramolecular array of polarized water, which constitutes a dynamic long-range multilayered structure of oriented dipoles, is cooperatively modulated by metabolic activity (e.g., ATP levels) through association and electronic inductive effects on the extended proteins themselves [22, 30]. It is very important to note that the dynamic nature of polarized water dipole networks entails changes in the rotational freedom of water molecules, affecting water chemical potentials (and consequently activity) and therefore provides a satisfactory explanation of the fluorescent response of ACDAN (and PRODAN) in the cell cytosol [19, 20, 23]. From these studies a mathematical model was devised by combining the Yang-Ling isotherm, which is entirely based on AIH principles, with kinetic schemes describing glycolysis [20, 23]. The model not only successfully reproduces the observed experimental coupling between ATP oscillations and intracellular water dynamics, but also predicts that metabolic modulation of the physical state of intracellular water can be propagated. This is done via water polarization from places where the chemical fluctuation in ATP occurs to others where this chemical process is absent, thus accounting for the cell-wide coupling of numerous variables [20, 23]. Overall, changes in water activity modulated by the metabolic state of the cell can easily influence not only enzymatic activity but also lipid structure by the phenomenon of lyotropic mesomorphism [28, 29, 31]. In our opinion all these considerations strongly support water dipolar relaxation, as sensed by the DAN probes, as a key measure of the states and dynamics of the intracellular environment.

3. Methods and applications reported for ACDAN in biological systems

After its first use as a probe to measure water dipolar relaxation in the cell cytosol of oscillating yeast cells (discussed in section 2.2 above), other studies using ACDAN have been conducted in diverse biological systems. Applications included measuring water dipolar relaxation in zebra fish lenses [32], metabolism-dependent water dynamics in the lumen of trafficking lysosomes [33] and water dipolar relaxation during formation of liquid droplets upon interaction of Zika and Dengue virus capsid proteins with nucleic acids [34]. The versatility of ACDAN has allowed examination of water dipolar relaxation in very specialized structures [32], metabolic states in cells [19, 20, 23] and their organelles [33], as well as the characterization of liquid condensates in biomimetic systems [34]. Rather than discussing the general scientific considerations concerning the distinct systems studied using ACDAN, this section will instead focus on the reported technical aspects of the methods. This includes labeling strategies, preferred fluorescent parameters measured and data analysis.

3.1 Fluorescent staining.

Specimen labeling procedures are very general and easily carried out: incorporation of ACDAN into the cell interior (or into liquid condensates) is attained by passive diffusion upon incubation with very concentrated solutions of the probe in DMSO (for details please see [19-21,23]). Stocks of up to 60 mM ACDAN (up to 40 mM PRODAN and 5 mM LAURDAN) are easily prepared, which allow incubation of the samples with very low volumes of DMSO for final probe concentrations in the micromolar range. In general, these micromolar concentrations are enough for measurements with adequate signal to noise ratios. The procedure limits the dose of organic solvent used but, in any case, control experiments using the organic solvent alone are always required.

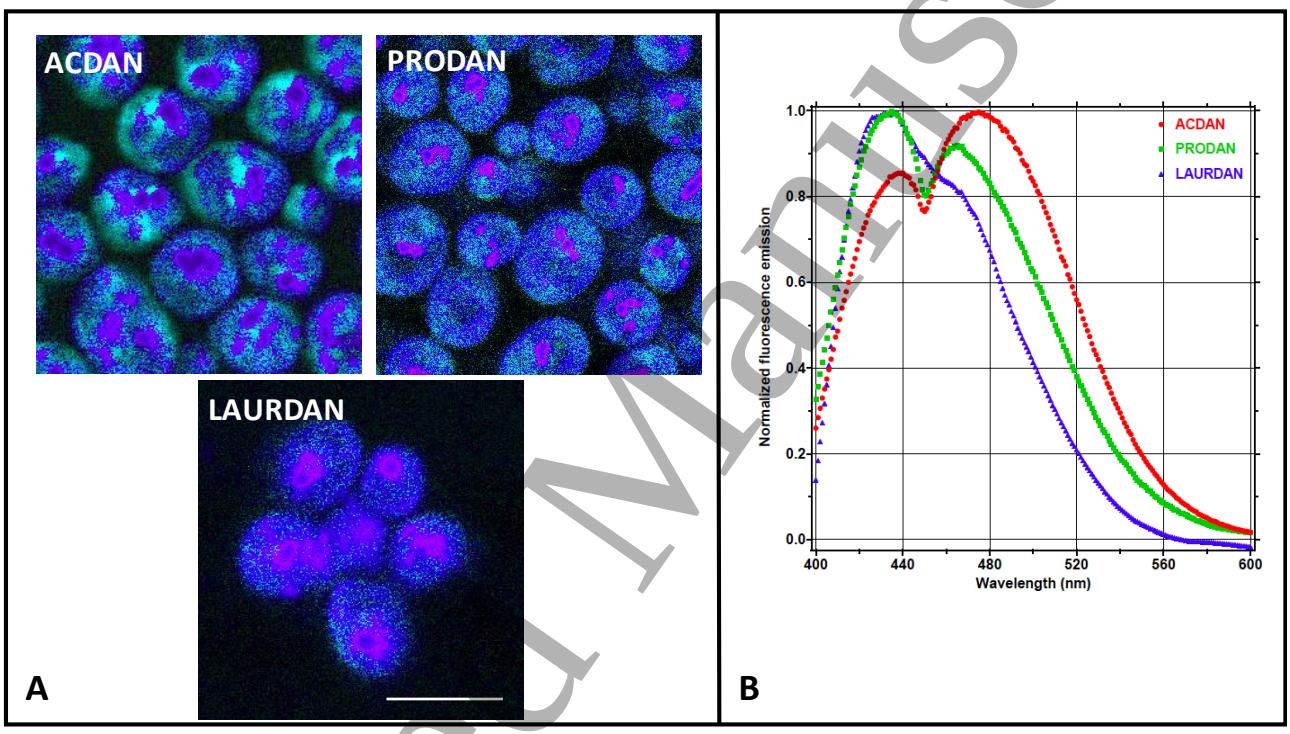

Figure 4. A) Spectral fluorescence images of ACDAN, PRODAN and LAURDAN in yeast cells. The color scale in the images corresponds to the wavelength range used in B; unrelaxed (violet), partially relaxed (blue) and relaxed (green) fluorescence emission areas, respectively. The scale bar is 5 μm. B) Emission spectra of fluorescently labeled yeast obtained in the fluorometer. The shapes of the different spectra reflect the heterogeneity of water dipolar relaxation observed in the cell interior. Adapted from [19].

As an example, Figure 4 shows spectral two photon excitation fluorescence microscopy images of *Saccharomyces cerevisiae* cells labeled with ACDAN, PRODAN and LAURDAN after 1 hour incubation with concentrated stocks in DMSO for final concentrations of 10 μM. As can be seen in Figure 4 the cell interior is labeled (except the vacuoles) showing heterogeneous dipolar relaxation evident from the color of the emission, which goes from violet (unrelaxed) to greenish (relaxed). In

addition, the different hydrophilic/hydrophobic balance of the probes impacts on their intracellular distribution, allowing mapping dipolar relaxation in different regions of the cell [19]. In these experiments autofluorescence was negligible.

3.2 Fluorescence measurements

As exemplified in previous sections, the preferred fluorescent parameter measured for ACDAN has been the fluorescence emission spectrum. Two different strategies are generally used to measure fluorescence emission: "bulk" type measurements using fluorometers [19-21] that allow fast time-resolved measurements and very fine spectral resolution, and fluorescence imaging using confocal fluorescence microscopy (one photon [33, 34] or multiphoton excitation [19, 32]), which allows spatially resolved information. In most applications mentioned above the emission spectra collected are analyzed in two ways: using the generalized polarization (GP) function or applying spectral phasor analysis.

3.2.1 GP function

The GP is a two-state model-based parameter that relies on the mechanism described in section 2.1. Defined by Parasassi et al. in the early '90s to study lipid membranes with LAURDAN (and PRODAN) [6, 7, 12], this parameter reflects the extent of water dipolar relaxation around the probe. This allows monitoring unrelaxed and relaxed environmental states that are connected to the thermodynamic phase state of the membrane. The GP function was defined analogously to the fluorescence polarization function as:

$$GP = \frac{I_B - I_R}{I_B + I_R} \qquad (1)$$

where I_B and I_R correspond to the intensities at the blue and red edges of the emission spectrum using a given excitation wavelength. In general, high GP values correspond to unrelaxed environments (emission enriched in shorter wavelengths) whereas low GP values correspond to relaxed surroundings around the probe (emission enriched in longer wavelengths). This parameter has been generalized for ACDAN [35] and used to measure dipolar relaxation in the cell cytosol [19-21] and organelles [33]. An example of ACDAN GP data obtained in a spectrofluorimeter is shown in Figure 3, where oscillation of this function is recorded during oscillating glycolysis in yeast cultures. Spatially resolved information can also be obtained using confocal fluorescence microscopy as shown by Begarani et al. in lysosomes from eukaryotic cells [33] and, as we will show in the next section,

in plant specimens. Several dedicated reviews have been published describing the uses of the GP function [10, 11]

3.2.2 Spectral phasor analysis

In contrast to the GP function, the spectral phasor method for the study of the emission of environmentally sensitive probes such as the DAN series is a fast and consistent method to approach complex processes without the necessity of models [36]. In this analysis the spectrum is transformed into a vector using the following expressions for *x* and *y* coordinates:

$$y = G_{(\lambda)} = \frac{\sum_\lambda F(\lambda)\cos\left(\frac{2\pi n(\lambda-\lambda_0)}{L}\right)}{\sum_\lambda F(\lambda)} \quad (2)$$

$$x = S_{(\lambda)} = \frac{\sum_\lambda F(\lambda)\sin\left(\frac{2\pi n(\lambda-\lambda_0)}{L}\right)}{\sum_\lambda F(\lambda)} \quad (3)$$

where $F(\lambda)$ are the fluorescence intensity values, λ_0 is the initial wavelength of the spectrum, L is the length of the spectrum and n is the harmonic value. The angular position of the phasor in the plot is related to the center of mass of the spectrum, while the radial position depends on its full width at half maximum (FWHM) [36]. In this analysis a point in the phasor plot corresponds to a defined "state" of the system. Given the vectorial properties of Fourier space and in a system with two components, when the phasors for the pure components are known then those of the mixtures will fall between them as linear combinations of the two reference states. As in the case of the GP function, phasor analysis can be achieved from data obtained in a fluorometer, or in a spectral fluorescence microscope with optical sectioning (confocal or multiphoton excitation). This has been exploited to characterize membrane phase transitions using LAURDAN [31, 37] and can be extended to experiments using ACDAN to relate trajectories between relaxed and unrelaxed states of, for example, regions of the crowded cytosol. As mentioned above the most important advantage of spectral phasor over GP analysis is that it is model-free [36]: it requires no assumptions on the many components or environments for ACDAN within complex systems (like cells or tissues), including autofluorescence.

As an interesting example, the application of the spectral phasor analysis in spectral images of ACDAN-labeled zebrafish lenses revealed that mutations in two zebrafish aquaporin 0 genes, Aqp0a and Aqp0b, alter the relaxation dynamics of water and macromolecular crowding in living lenses,

producing cataracts and blindness [32]. The effect of crowding as observed in the phasor plot is illustrated in Figure 5 from solutions containing Antarctic tooth fish γM8d crystallin at concentrations of 0, 85, 140, 216, 264, and 340 mg/ml. A blue spectral shift is observed in response to increased macromolecular crowding, which corresponds to a clockwise displacement of the phasor as the concentration increases.

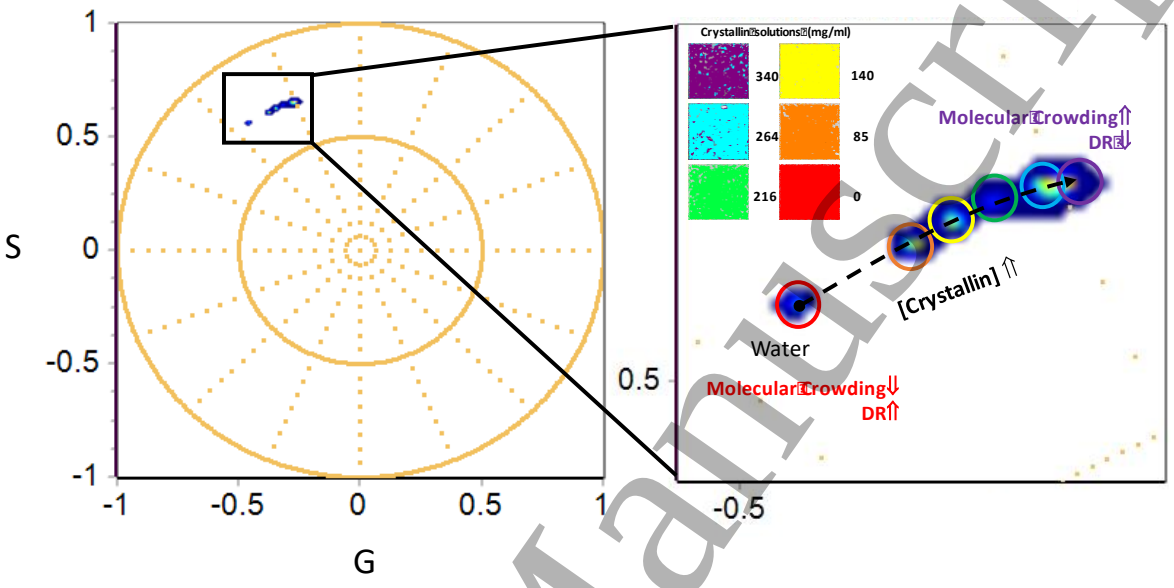

Figure 5. Phasor plot of spectral emission of ACDAN in solutions containing Antarctic toothfish crystalline protein at different concentrations. A blue spectral shift is observed in response to increased macromolecular crowding. Inset showing the spectral phasor space with the region of interest indicated as a black square of the left figure. Circles used at different protein concentrations follow the color coding of the images in the top left inset. Adapted from [32]

The ACDAN naked emission spectrum has also been used to study water relaxation during formation of liquid droplets (or liquid-liquid phase separation). These droplets, which are formed upon interaction of Zika and Dengue virus capsid proteins with nucleic acids, exhibit blue-shifted ACDAN emission when compared to their surroundings, signaling a decrease in water relaxation inside the droplets [34]. These experiments show that water relaxation, and consequently its activity, changes in the coacervate with potential effects on local enzymatic activity and/or membrane mesomorphism. This may be of relevance since the formation of these coacervates (often called liquid condensates) has been proposed to play a crucial role in the assembly of, for example, highly dynamic organelles such as the Golgi complex [38], whose surface has been generally portrayed as membrane-bound, that is, delimited by what are now understood as “classical” lipid bilayers. The regulation of water activity in this case could lead to the transient formation of highly curved non-lamellar phases explaining transitions to highly curved (dynamical) states of the organelle during the cell cycle.

The next section will present novel data applying the ACDAN method in plant cells and tissues. Again, this information is mainly methodological and discusses technical details of the experiments.

4. Novel applications of ACDAN in plant cells and tissues

4.1 Material and Methods

4.1.1. Materials

ACDAN was purchased from Santa Cruz Biotechnology Inc. Dimethyl sulfoxide (DMSO) was of analytical grade (Sintorgan, Argentina). 4-Morpholineethanesulfonic acid (MES) was purchased from Sigma-Aldrich, Buenos Aires, Argentina.

4.1.2. Plant Growth Conditions

Seeds of *Arabidopsis thaliana* ecotype Columbia (Col-0) were surface-sterilized and sown on plates containing Murashige & Skoog medium (MS, Duchefa Biochemie), containing 0.8 % agar (Britania) and pH 5.8 After sowing, plates were kept in darkness at 4°C for 2 days, and then transferred to a growth chamber. Experiments were conducted under a 16 h light/8 h dark photoperiod. Photosynthetic photon flux density was 100 μmol m^{-2} sec^{-1}. Average temperature was 22°C (day) and 18°C (night). Plants were grown for 3-4 days under these conditions.

4.1.3. ACDAN Staining

Plants were submerged in 60 μM ACDAN aqueous solution, incubated for 2 h at 25 °C and washed twice with distilled water. Plants were then mounted in glass slides containing MS 0.5X with 10 mM MES and pH 5.8 for microscope observation.

4.1.4. Microscopy measurements and analysis

Fluorescence images were obtained using an Olympus FV1200 laser-scanning confocal microscope. The fluorescence signal was collected through a 60X immersion silicone objective (UPLSAPO 60X S, NA 1.3). For spectral images, ACDAN was excited with a 405 nm laser, excitation dichroic mirror BS20/80 and fluorescence emission was detected between 420 and 600 nm, with a resolution of 10 nm. For GP images, ACDAN was excited with 405 nm laser, excitation dichroic mirror 405/473 and detector filters 425-500 nm (blue) and 525-560 nm (green). Autofluorescence in these conditions was negligible. Spectral data were processed using the SimFCS software (LFD, Irvine, CA). GP analysis was carried out with a Generalized Polarization Analysis Plugin developed by Bob Dougherty (https://www.optinav.info/Generalized_Polarization_Analysis.htm), of ImageJ version 1.53q (National Institute of Health, USA). GP images were corrected using a G-factor obtained with a standard solution in DMSO (60 μM) according to [39].

4.2 Results and discussion

To further examine the usefulness of the method, ACDAN experiments were performed in photosynthetic (cotyledons) and non-photosynthetic (root) tissues of living *Arabidopsis thaliana*. Figure 6 shows ACDAN fluorescence images from cotyledon epidermis and from apical and elongation zones of root tissue.

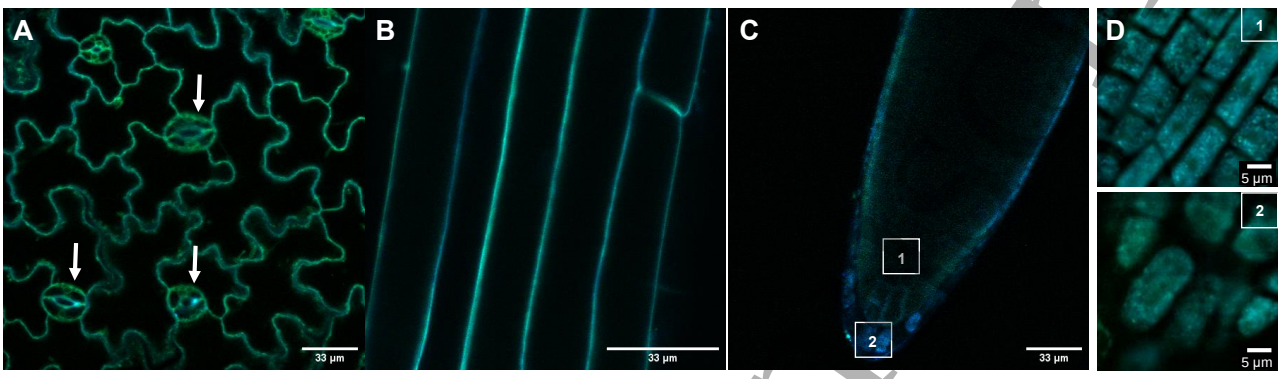

Figure 6. Confocal fluorescence images of ACDAN labeled (4 days) living *Arabidopsis thaliana* plants. A) Epidermis, B) Root elongation zone and C) apical root. D) ROI 1 and ROI 2 of the apical root as indicated with the white squares in the figure are enlarged in D. The white arrows in A indicate stomata. The emission intensity images merge the blue and green fluorescence channels (for details see material and methods section).

The images show that ACDAN is excluded from the inner volume of the vacuoles, preferentially labeling the periphery of the cell. This would likely include regions of the cell cytosol, the cell wall and the plasma membrane, discrimination of which is not possible because of the limited radial resolution of 250 nm. The unlabeled vacuoles in the cells of the cotyledon epidermis and in the root elongation zone occupy most of the cell volume (Figure 6 A and B). In contrast, cells of the apical region –that is, the meristematic zone (Figure 6 C- ROI 1) and the root cap (Figure 6 C-ROI 2)– contain vacuoles that are much smaller relative to cytosolic volume (Figure 6D). Whereas the vacuole can occupy up to 95% of the volume of a mature cell, meristematic cells have many small vacuoles that eventually fuse to give rise to it. Stomata (guard cells + stomatal pore) in the cotyledon's epidermis are also clearly labeled (white arrows in Figure 6A).

Besides the morphological information provided by ACDAN fluorescence images, the sensitivity of the probe to water dipolar relaxation can also be exploited for GP and spectral phasor analyses. A first example is shown for the stoma in Figures 7 and 8.

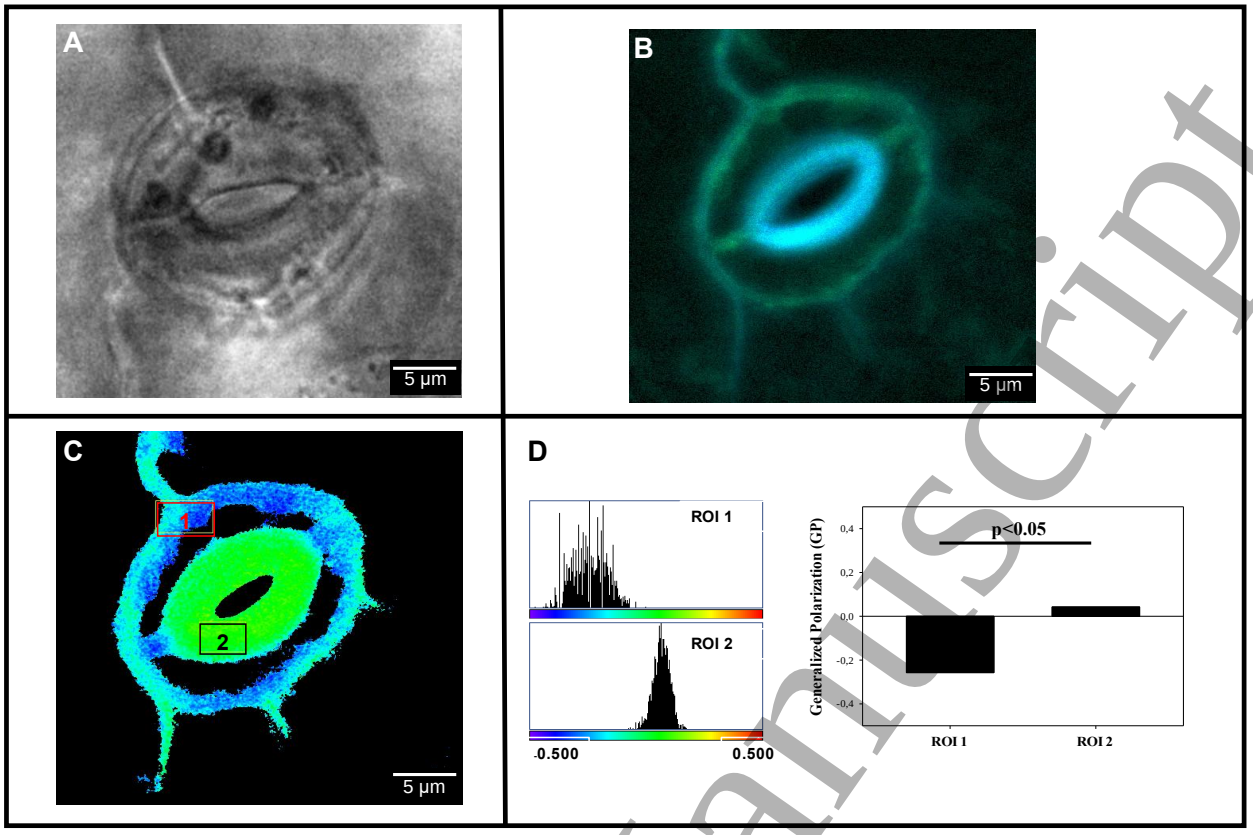

Figure 7. ACDAN GP analysis of a stoma. (A) Transmission microscopy image, (B) confocal fluorescence microscopy image (merge of blue and green intensity channels), (C) GP image. Two ROIs were selected from (C) corresponding to areas of high (1) and low (2) dipolar relaxation. GP-histogram of ROI 1 and 2 and a student t-test analysis are shown in (D). GP of the ROIs were mean ± SD. $p < 0.05$ indicates significant differences between the two regions.

Figures 7A and B respectively show transmission and fluorescence intensity images of a stoma. The fluorescence intensity images obtained with the two bandpass filters were used to compute the GP image (Figure 7C) by applying equation 1. Two distinct GP regions are apparent: the inner (ROI 2) (facing the pore) and the outer faces (ROI 1) of the guard cells, respectively. Dipolar relaxation in the outer face is significantly lower than in the inner face of the guard cells, as indicated by the ROI's GP distributions and statistical analysis presented in Figure 7D.

Figure 8 summarizes the phasor analysis of the stoma using the spectral fluorescence image to compute the spectral phasor plot by means of equations 2 and 3 (Figure 8A).

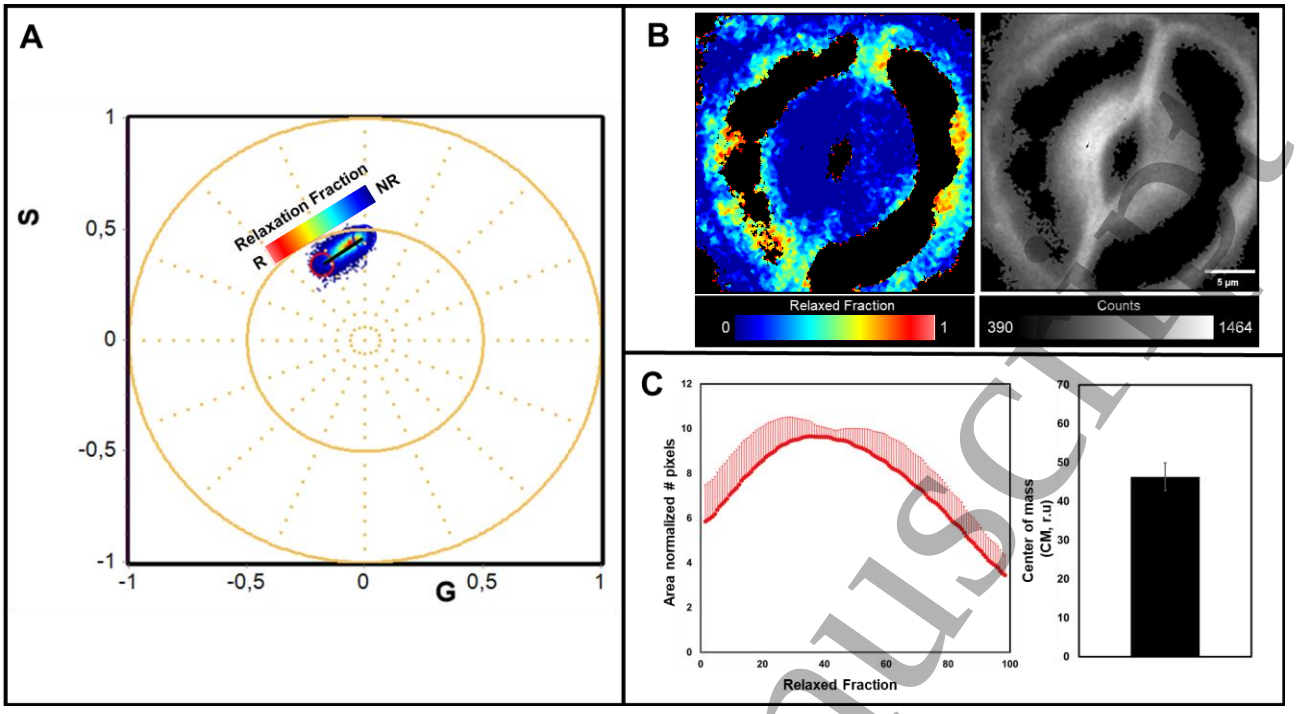

Figure 8. Spectral phasor plot distribution (A) and spectral phasor image (B, left) for the stoma. In (B) the corresponding fluorescence intensity image is included (right). A two-component analysis -relaxed (R) and non-relaxed (NR)- was performed and the R fraction calculated. The spectral phasor image was colored using the R-fraction color scale indicated in (A). C) A histogram for the R-fraction was generated using images of several stomata (n=9). Then the average and standard deviation were calculated. Data are presented as mean+SD. Negative standard deviation was avoided to simplify the plots. The bar plot in the right indicates the center of mass of the histogram (as mean±SD).

The spectral phasor plot contains a distribution of phasors generated from pixels with distinct emission spectra (that is, relaxation). The extremes of the black ruler in Figure 8A represent the relaxed and non-relaxed pixels and are indicated by the red and blue circles, respectively. The linear trajectory between these two points suggests the existence of two single environments for ACDAN characterized by “relaxed” and “non-relaxed” water, with the intermediary points of the trajectory showing linear combinations of these two states. Using a two-component analysis it is then possible to calculate the fraction of relaxed and non-relaxed pixels in the image, as shown in Figure 8C. In line with the GP analysis, the color code used for the phasor image (Figure 8B, left) shows that the extent of dipolar relaxation in the outer face is significantly greater than that observed in the inner face of guard cells. It is reasonable to suppose that this "water architecture" of the stoma is not accidental and may have important functional implications in plant physiology, since stomata are the main regulated resistance for gaseous exchange, loss of water vapor by transpiration and entrance of carbon dioxide to sustain photosynthesis. Stomatal resistance is regulated by opening and closing the

stomatal pore, operated by the guard cells, which have thickened cell walls (mainly the inner face) with a particular cellulose microfilm disposition. The opening and closing of the stomatal pore is modulated by many environmental factors and motorized by water chemical potential changes and, consequently, the turgor pressure of the guard cells [40]. This is congruous with the peculiar spatial distribution of dipolar relaxation measured by ACDAN, showing that this parameter can be useful to differentiate singular structures and, possibly, functional states in given tissues or cells (e.g. time-resolved studies of the changes in relaxation as stomata open and close, etc).

Our second example compares GP images between different zones of non-photosynthetic tissues (apical, meristematic and elongation zones of the root). This analysis is shown in Figure 9.

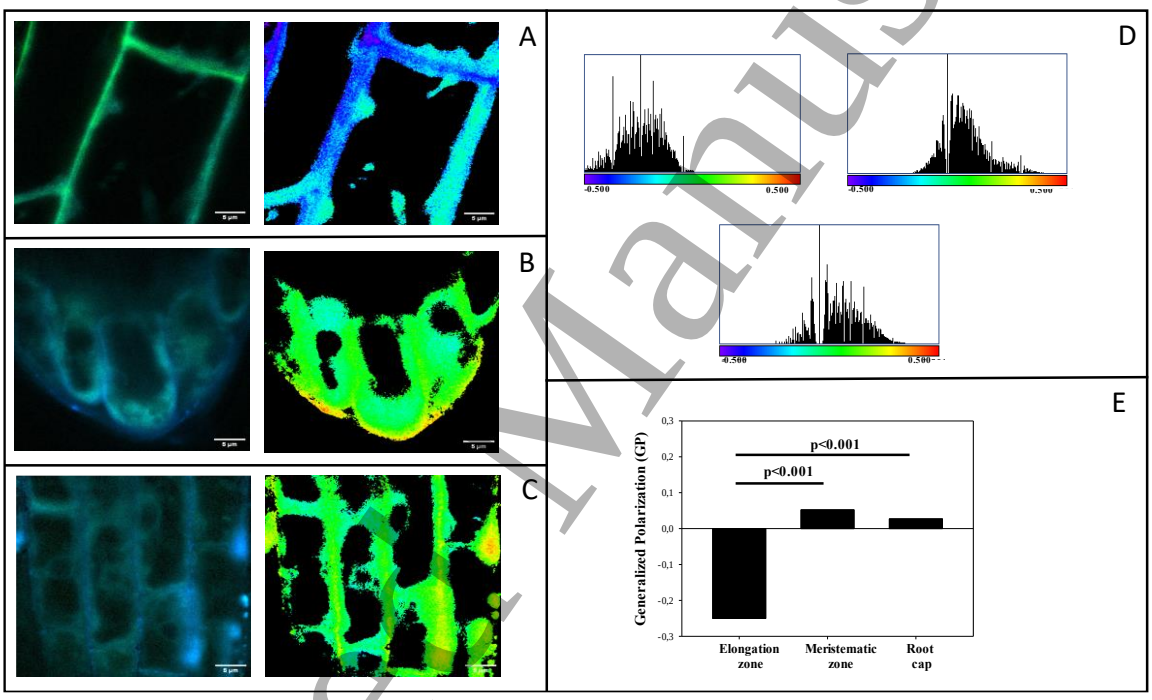

Figure 9. ACDAN GP analysis of the root. Confocal fluorescence intensity (left) and GP (right) images of elongation (A), meristematic (B) and root cap (C) zones of root. (D) GP-histograms of elongation zone (top left), meristematic zone (top right) and root cap (bottom) of apical root. (E) GP of the elongation zone, root cap and meristematic zone of apical root as mean±SD. The ANOVA p-values shown in the graph indicate differences between the elongation zone and different parts of the apical root.

From the results it can be seen that the GP measured in the apical zone of the root (root cap and meristematic zones, Figures 9B and C respectively) is conspicuously higher than in the elongation zone (Figure 9A), indicating very different degrees of dipolar relaxation in each. The GP model can partially show different local relaxation states based on a two-state model and, with proper

calibrations using the G-factor (see material and methods), comparisons among different structures can be reliably made.

A comprehensive comparison of the whole sample -which would include photosynthetic (stoma) and non-photosynthetic regions (elongation zone, root cap and meristematic zone of apical root)- can be done, however, using the phasor plot analysis. The analysis requires first defining the extremes of the distributions of the whole phasor plot by simultaneous analysis of all phasor images. From this operation it is clear that the distribution is not reducible to just two components as the one shown in Figure 8 (compare Figures 8A and 10A). This deviation originates particularly from the distribution reflecting the elongation zone of the root (see Figure 10A, blue cloud near the blue circle) and requires a three-component analysis [41]. This analysis is performed by constructing a triangle between the original trajectory for relaxed and non-relaxed water environments and a 3rd component which we place in S,G (0,0). Using a three-cursor analysis it is then possible to calculate the relaxed and non-relaxed fractions taking into account the pixels under the linear combination, along with a third component we do not yet know the origin of (Fig. 10A). The reason of the (0,0) selection as the 3rd component is to use this analysis to quantify the spectral shift (relaxation) as a phase increase, and the spectral broadening (3rd component) as a decrease in the modulation. By using this approach, relaxation across the whole plant specimen can be consistently compared.

The elongation zone shows increased relaxation in comparison to the other plant structures while the meristematic region and the root cap display similar intermediate dipolar relaxation values (Figures 10C and E). The use of the 3rd component enables identification (and quantitation) of this highly relaxed component between the different structures. Noticeably, it becomes evident only in the elongation zone (Figure 10D) since stomata, meristematic regions and root caps all fall on the line defined by linear combinations of just two components (relaxed and non-relaxed). Of all the structures the stomata display the lowest dipolar relaxation.

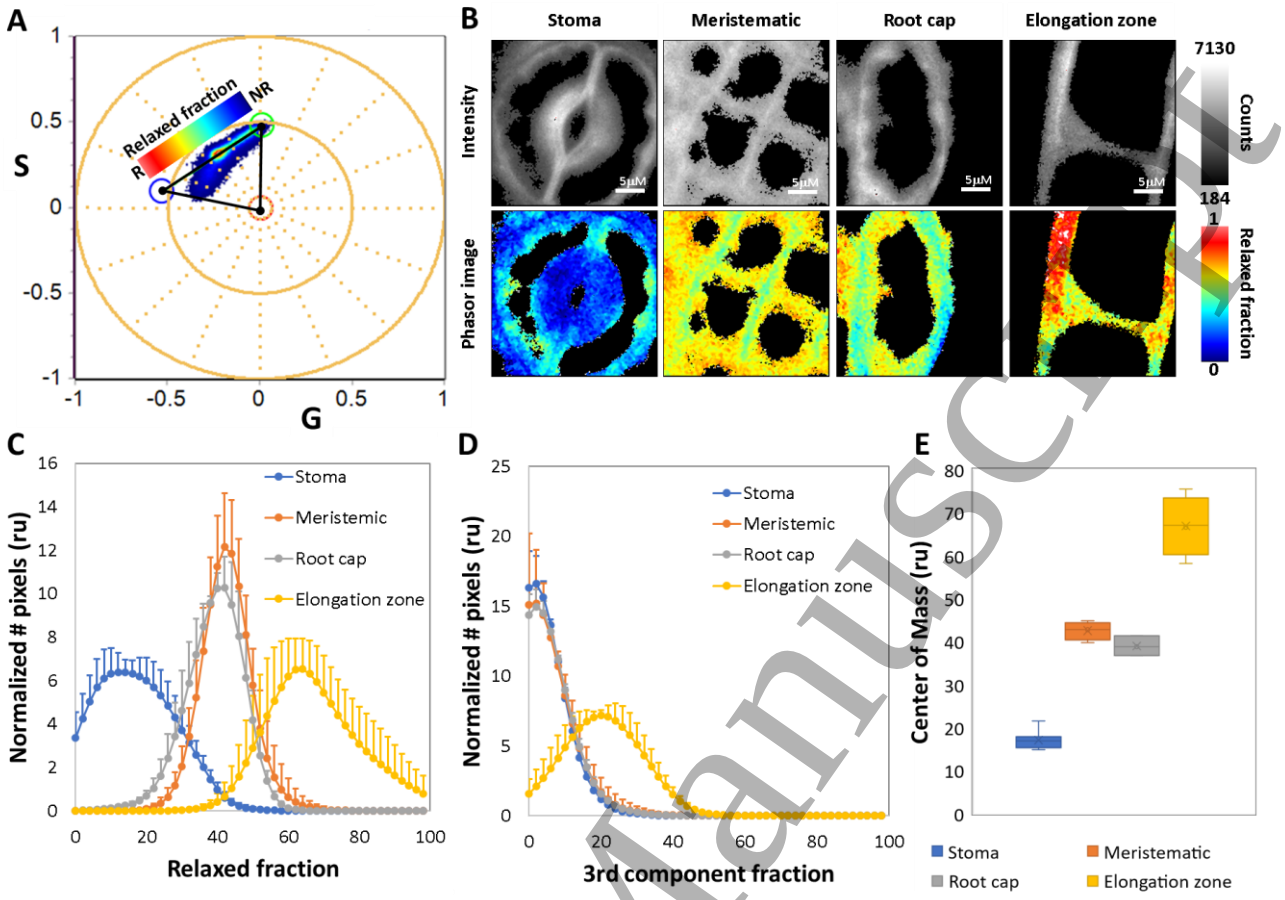

Figure 10. Spectral phasor plot (A), and intensity/spectral phasor images (B) for different parts of the root and a stoma. A two-component analysis -relaxed (R) and non-relaxed (NR)- was performed. In B different parts of the root were colored using the color scale denoting the R-fraction. C) A histogram for the relaxed fraction was generated using different images (n=20) by calculation of the average and standard deviation. D) A histogram for the third component fraction was generated using different images (n=20) by calculation of the average and standard deviation. For the relaxed fraction and third component fraction the data are presented as mean+SD. E) Center of mass plot for relaxed fraction histogram to quantitatively compare different parts of the root and stoma (as mean±SD).

From our observations, it is not unreasonable to surmise that these differences concerning the 3rd-component arise from different metabolic states of the root zones, where the cells growing by a process of elongation actively incorporate water to the vacuole. This differs between undifferentiated cells (meristematic zone) and root cap zone differentiated cells with protection and perception functions. In fact, although further studies are needed it, this 3rd-component can be reasonably modeled with the position of ACDAN in free water as we indicate in Figure 11. In other words, using the advantages of the model-free approach of phasors we can hypothesize that the elongation zone of

the root is characterized by fractions of the environment experimented by ACDAN in the apical root (meristematic and cap root zones) and in "free" water.

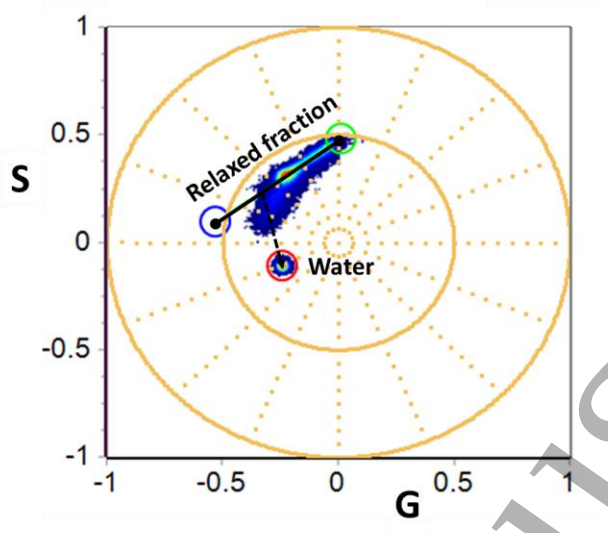

Figure 11. Spectral phasor plot for ACDAN data from different parts of the root and stoma. ACDAN in water was include. Notice the third component form elongation zone is pull toward to ACDAN in pure water.

To the best of our knowledge this is the first time that ACDAN has been used to study dipolar relaxation in photosynthetic and non-photosynthetic tissues of plants. Only two previous applications were found in plant specimens using a DAN fluorescent probe, LAURDAN, which exclusively focused on membrane studies. One explored the presence of sphingolipid-enriched plasma membrane domains in *Arabidopsis thaliana* protoplasts using fluorescence microscopy [42] while the other studied changes in fluidity in thylakoid membranes [43]. On the use of polarity sensitive fluorophores other than DAN in plant tissues, we found a report describing the synthesis of 1-(2-acryloyloxy-3-chloro-prop-1-yl)-amino-5-isocyanonaphthalene (ACAIN) [44]. ACAIN, which was inspired by ACRYLODAN [3] (another DAN derivative), can be covalently attached to free thiol groups in proteins. Applications of ACAIN in living *Arabidopsis thaliana* showed that it preferentially labels proteins in the tonoplasts [45]. In that study, however, its solvatochromic properties were not exploited, as the study was limited to the use of whole fluorescence emission for colocalization studies with GFP constructs.

5. Conclusions

This article reviews examples and technical aspects of a new analytical method using the ACDAN probe. As a member of the DAN series the probe is sensitive to the extent of water dipolar relaxation

and, consequently, water activity. The dynamical state of water in the environment of the probe is shown to provide valuable information on the cell interior as discussed in section 2 and, with a proper theoretical framework such as the AIH, can operate as a surrogate marker for the functional and/or metabolic state of tissues, cells and subcellular structures in widely different biological systems (yeast, plants and animals). This novel methodology considerably extends Weber's original proposal of these fluorophores as "relaxation probes of various biological environments" [1] into a general tool to study the complex, crowded and dynamic cellular interior underlying numerous specific activities and functions of cells. The dipolar relaxation parameter can not only help differentiate singular structures in a given tissue or cell, but can also be used to characterize another layer of complexity in the functional responses of specimens to perturbations of metabolic, chemical, physical and physiological origin.

Acknowledgments:

The authors have declared that no conflicting interests exist. LM is supported as Imaging Scientist by grant number 2020-225439 and the grant "Expanding Global Access to Bioimaging RFA" from the Chan Zuckerberg Initiative DAF, an advised fund of Silicon Valley Community Foundation. RL is funded by grants from Agencia Nacional de Promoción de aa Investigación, el Desarrollo Tecnológico y la Innovación (PICT 2019-00533) INTA (2019-PD-E4-I085, P01), CONICET (PIP 2015 y 2020), Secretaria de Ciencia y Técnica de la Universidad nacional de Córdoba, Ministerio de Ciencia y Tecnología de Córdoba; LB was funded by Agencia Nacional de Promoción de Investigación, el Desarrollo Tecnológico y la Innovación (PICT 2017-2658 y 2019-00471)

References

[1] G. Weber, F.J. Farris, Synthesis and spectral properties of a hydrophobic fluorescent probe: 6-propionyl-2-(dimethylamino)naphthalene, Biochemistry, 18 (1979) 3075-3078.
[2] R.B. Macgregor, G. Weber, Estimation of the polarity of the protein interior by optical spectroscopy, Nature, 319 (1986) 70-73.
[3] F.G. Prendergast, M. Meyer, G.L. Carlson, S. Iida, J.D. Potter, Synthesis, spectral properties, and use of 6-acryloyl-2-dimethylaminonaphthalene (Acrylodan). A thiol-selective, polarity-sensitive fluorescent probe, J. Biol. Chem., 258 (1983) 7541-7544.
[4] T. Parasassi, F. Conti, E. Gratton, Fluorophores in a polar medium: time dependence of emission spectra detected by multifrequency phase and modulation fluorometry, Cellular and molecular biology, 32 (1986) 99-102.

[5] T. Parasassi, F. Conti, E. Gratton, Time-resolved fluorescence emission spectra of Laurdan in phospholipid vesicles by multifrequency phase and modulation fluorometry, Cellular and molecular biology, 32 (1986) 103-108.
[6] T. Parasassi, G. De Stasio, A. d'Ubaldo, E. Gratton, Phase fluctuation in phospholipid membranes revealed by Laurdan fluorescence, Biophys J, 57 (1990) 1179-1186.
[7] T. Parasassi, G. De Stasio, G. Ravagnan, R.M. Rusch, E. Gratton, Quantitation of lipid phases in phospholipid vesicles by the generalized polarization of Laurdan fluorescence, Biophys J, 60 (1991) 179-189.
[8] T. Parasassi, E. Gratton, Packing of phospholipid vesicles studied by oxigen quenching of Laurdan fluorescence, J. Fluorescence, 2 (1992) 167-174.
[9] T. Parasassi, E. Gratton, W.M. Yu, P. Wilson, M. Levi, Two-photon fluorescence microscopy of laurdan generalized polarization domains in model and natural membranes, Biophys. J., 72 (1997) 2413-2429.
[10] T. Parasassi, E.K. Krasnowska, L. Bagatolli, E. Gratton, LAURDAN and PRODAN as polarity-sensitive fluorescent membrane probes, Journal of fluorescence, 8 (1998) 365-373.
[11] L.A. Bagatolli, LAURDAN fluorescence properties in membranes: a journey from the fluorometer to the microscope, in: Y. Mely, G. Duportail (Eds.) Fluorescent Methods to study Biological Membranes, vol. 13, Springer-Verlag, Heidelberg, 2013.
[12] E.K. Kranowska, E. Gratton, T. Parasassi, Prodan as membrane surface fluorescence probe: partitioning between water and phospholipid phases, Biophys. J., 74 (1998) 1984-1993.
[13] J.R. Lakowicz, D.R. Bevan, B.P. Maliwal, H. Cherek, A. Balter, Synthesis and characterization of a fluorescence probe of the phase transition and dynamic properties of membranes, Biochemistry, 22 (1983) 5714-5722.
[14] P. Jurkiewicz, J. Sykora, A. Olzynska, J. Humpolickova, M. Hof, Solvent relaxation in phospholipid bilayers: principles and recent applications, Journal of fluorescence, 15 (2005) 883-894.
[15] H.M. Kim, H.J. Choo, S.Y. Jung, Y.G. Ko, W.H. Park, S.J. Jeon, C.H. Kim, T. Joo, B.R. Cho, A two-photon fluorescent probe for lipid raft imaging: C-laurdan, Chembiochem, 8 (2007) 553-559.
[16] M.M. Dodes Traian, L. Gonzalez Flecha, V. Levi, Imaging lipid lateral organization in membranes with C-laurdan in a confocal microscope, J Lipid Res, (2011).
[17] G. Bianchetti, S. Azoulay-Ginsburg, N.Y. Keshet-Levy, A. Malka, S. Zilber, E.E. Korshin, S. Sasson, M.D. Spirito, A. Gruzman, G. Maulucci, Investigation of the Membrane Fluidity Regulation of Fatty Acid Intracellular Distribution by Fluorescence Lifetime Imaging of Novel Polarity Sensitive Fluorescent Derivatives, Int. J. Mol. Sci. , 22 (20121) 3106.
[18] J. Zeng, P.L. Chong, Effect of ethanol-induced lipid interdigitation on the membrane solubility of Prodan, Acdan, and Laurdan, Biophys J, 68 (1995) 567-573.
[19] H.S. Thoke, A. Tobiesen, J. Brewer, P.L. Hansen, R.P. Stock, L.F. Olsen, L.A. Bagatolli, Tight Coupling of Metabolic Oscillations and Intracellular Water Dynamics in Saccharomyces cerevisiae, PloS one, 10 (2015) e0117308.
[20] H.S. Thoke, S. Thorsteinsson, R.P. Stock, L.A. Bagatolli, L.F. Olsen, The dynamics of intracellular water constrains glycolytic oscillations in Saccharomyces cerevisiae, Scientific Reports, 7 (2017) 16250.
[21] L.F. Olsen, R.P. Stock, L.A. Bagatolli, Glycolytic oscillations and intracellular K+ concentration are strongly coupled in the yeast Saccharomyces cerevisiae, Arch. Biochem. Biophys, 681 (2020) 108257.
[22] G.N. Ling, Life at the cell and below cell level. The hidden history of a fundamental revolution in biology, Pacific Press, 2001.

[23] H.S. Thoke, L.A. Bagatolli, L.F. Olsen, Effect of macromolecular crowding on the kinetics of glycolytic enzymes and the behaviour of glycolysis in yeast, Integr. Biol., 10 (2018) 587-597.
[24] H.S. Thoke, L.F. Olsen, L. Duelund, R.P. Stock, T. Heimburg, L.A. Bagatolli, Is a constant low-entropy process at the root of glycolytic oscillations? , Journal of Biological Physics, 44 (2018) 419-431.
[25] J. Lara-Popoca, H.S. Thoke, R.P. Stock, E. Rudino-Pinera, L.A. Bagatolli, Inductive effects in amino acids and peptides: effects in ionization constants and tryptophan fluorescence, Biochemistry and Biophysics Reports, 24 (2020) 100802.
[26] E. Lippert, Spektroskopische Bestimmung des Dipolmomentes aromatischer Verbindungen im ersten angeregten Singulettzustand, Z. Elektrochem., 61 (1957) 962-975.
[27] G.N. Ling, A physical theory of the living state: the Association-induction hypothesis. , Blaisdell Publishing Co., New York, 1962.
[28] L.A. Bagatolli, R.P. Stock, Lipid, membranes, colloids and cells. A long view, Biochim Biophys Acta - Biomembranes, 1863 (2021) 183684.
[29] L.A. Bagatolli, R.P. Stock, L.F. Olsen, Coupled response of membrane hydration with oscillating metabolism in live cells: an alternative way to modulate structural aspects of biological membranes?, Biomolecules, 9 (2019) 687.
[30] G.N. Ling, A new theoretical foundation for the polarized-oriented multilayer theory of cell water and for inanimate systems demonstrating long-range dynamic structuring of water molecules, Physiol. Chem. Phys. & Med. NMR, 35 (2003) 91-130.
[31] A. Mangiarotti, L.A. Bagatolli, Impact of macromolecular crowding on the mesomorphic behaviour of lipid self-assemblies, Biochim. Biophys. Acta – Biomembranes, 1863 (2021) 183728.
[32] I. Vorontsova, A. Vallmitjana, B. Torrado, T.F. Schilling, J.E. Hall, E. Gratton, L. Malacrida, In vivo macromolecular crowding is differentially modulated by aquaporin 0 in zebrafish lens: Insights from a nanoenvironment sensor and spectral imaging, Sci. Adv., 8 (2022) eabj4833.
[33] F. Begarani, F. D'Autilia, G. Signore, A.D. Grosso, M. Cecchini, E. Gratton, F. Beltram, F. Cardarelli, Capturing Metabolism-Dependent Solvent Dynamics in the Lumen of a Trafficking Lysosome, ACS Nano, 13 (2019) 1670−1682.
[34] E.E. Ambroggio, G.S.C. Navarro, L.B.P. Socas, L.A. Bagatolli, A.V. Gamarnik, Dengue and Zika virus capsid proteins bind to membranes and self-assemble into liquid droplets with nucleic acids, J. Biol. Chem., 297 (2021) 101059.
[35] L.A. Bagatolli, R.P. Stock, The Use of 6-Acyl-2-(Dimethylamino)Naphthalenes as Relaxation Probes of Biological Environments, in: D.M. Jameson (Ed.) Perspectives on Fluorescence: A Tribute to Gregorio Weber, Springer, 2016, pp. 197-216.
[36] L. Malacrida, E. Gratton, D.M. Jameson, Model-free methods to study membrane environmental probes: a comparison of the spectral phasor and generalized polarization approaches, Methods Appl Fluoresc., 3 (2015) 047001.
[37] L. Malacrida, S. Astrada, A. Briva, M. Bollati-Fogolin, E. Gratton, L.A. Bagatolli, Spectral phasor analysis of LAURDAN fluorescence in live A549 lung cells to study the hydration and time evolution of intracellular lamellar body-like structures, Biochim Biophys Acta, 1858 (2016) 2625-2635.
[38] J.E. Rothman, Jim's View: Is the Golgi stack a phase-separated liquid crystal?, FEBS Letters, 593 (2019) 2701-2705.
[39] J. Brewer, J.B.d.l. Serna, K. Wagner, L.A. Bagatolli, Multiphoton excitation fluorescence microscopy in planar membrane systems, Biochimica et biophysica acta, 1798 (2010) 1301–1308.
[40] L. Taiz, E. Zeiger, Plant Physiology, 5th ed., Sinauer Associates Inc, Sunderland 2010.

[41] L. Malacrida, E. Gratton, LAURDAN fluorescence and phasor plots reveal the effects of a H2O2 bolus in NIH-3T3 fibroblast membranes dynamics and hydration, Free Radical Biology and Medicine, 128 (2018) 144-156.
[42] J.O. Blachutzik, F. Demir, I. Kreuzer, R. Hedrich, G.S. Harms, Methods of staining and visualization of sphingolipid enriched and non-enriched plasma membrane regions of Arabidopsis thaliana with fluorescent dyes and lipid analogues, Plant Methods, 8 (2012) 28.
[43] M. Bykowsk, R. Mazur, J. Wójtowicz, S. Suski, M. Garstka, A. Mostowska, Ł. Kowalewska, Too rigid to fold: Carotenoid-dependent decrease in thylakoid fluidity hampers the formation of chloroplast grana, Plant Physiol. , 185 (2021) 210–227. .
[44] M. Nagy, D. Racz, Z.L. Nagy, T. Nagy, P.P. Feher, M. Purgel, M. Zsuga, S. Keki, An acrylated isocyanonaphthalene based solvatochromic click reagent: Optical and biolabeling properties and quantum chemical modeling, Dyes and Pigments, 133 (2016) 445-457.
[45] M. Nagy, S. Kéki, D. Rácz, J. Mathur, G. Vereb, T. Garda, M. M-Hamvas, F. Chaumont, K. Bóka, B. Böddi, C. Freytag, G. Vasas, C. Máthé, Novel fluorochromes label tonoplast in living plant cells and reveal changes in vacuolar organization after treatment with protein phosphatase inhibitors, Protoplasma, 255 (2018) 829–839.